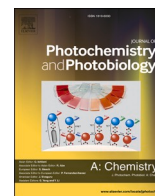




Contents lists available at ScienceDirect

Journal of Photochemistry & Photobiology, A: Chemistry

journal homepage: www.elsevier.com/locate/jphotochem

Synthesis of phthalimides, isoindolin-1-ones and isoindolines bearing aminobenzoic acids as a new fluorescent compounds

Melchor Solis-Santos^a, Mario Ordóñez^{a,*}, Adrián Ochoa-Terán^b, Rodrigo Morales-Cueto^a, Victoria Labastida-Galván^a

^a Centro de Investigaciones Químicas-IICBA, Universidad Autónoma del Estado de Morelos, Av. Universidad 1001, 62209, Cuernavaca, Morelos, Mexico

^b Centro de Graduados e Investigación en Química, Tecnológico Nacional de México/Instituto Tecnológico de Tijuana, Tijuana, B.C., Mexico

ARTICLE INFO

Keywords:

Phthalimides
isoindolin-1-ones
Isoindolines
Fluorescence
Absorption and emission

ABSTRACT

Both experimental and theoretical methods were used in order to study the fluorescent properties of nine new compounds based on phthalimides, isoindolin-1-ones and isoindolines bearing aminobenzoic acids (2-aminobenzoic acid, 3-aminobenzoic acid and 4-aminobenzoic acid), which were obtained under mild reaction conditions. The photophysical properties of all the compounds were studied by electronic absorption and fluorescence spectroscopy in methanol solutions. All compounds exhibited fluorescence emission and high quantum yields. Additionally, it was found that the intramolecular charge in these donor-acceptor systems is significantly depending on electron-withdrawing substituents at the carboxylic acid position.

1. Introduction

In the last two decades, the compounds with fluorescence properties have played a key role as analytical and diagnostic tools in organic and medicinal chemistry [1,2]. These compounds also called as chemosensors and fluorescent biomarkers [3–6], have been used to detect diseases, sense metal ions or imprint cellular marking to follow up the mechanisms that occur within them, consequently this area have received considerable attention due to the significant applications in several research fields such as medicine, molecular and cellular biology, biophysics, biotechnology and environmental sciences [7–9]. Despite the efforts made to develop fluorescent compounds with higher quantum yield and specificity, most of the obtained compounds show a high structural complexity and synthesis. One of the challenges resides on the creation of a non-toxic sensor that brings high effectiveness, sensitivity and an easy homogeneous association with substrates of different nature. Donor-acceptor (DA) compounds [10] have recently attracted technological and academic research, since they are increasingly finding applications in molecular electronics and optoelectronics, including organic light-emitting diodes (OLEDs) [11,12], electrogenerated chemiluminescence (ECL) [13,14], photovoltaic devices [15], biochemical fluorescence technology [16] and nonlinear optics [17].

Additionally, heterocyclic compounds containing heteroatoms such as nitrogen are considered as the most abundant molecular structures in

different natural and synthetic products [18]. Among these compounds, the phthalimide, isoindolin-1-one and isoindoline cores are of great importance as drugs and building blocks [19–21] in the preparation of compounds with a wide range of pharmacological activities, acting as antiviral [22], antimicrobial [23], antipsychotic [24] and antitumoral agents [25].

On the other hand, the phthalimides and isoindolin-1-ones are compounds with interesting photophysical properties [26–29]. Their versatility depends on the chromophore groups and auxochromes that these compounds possess, by favoring their different applications in the absorption of multi-photons, organic field effect transistors (OFET), organic light emitting diodes (OLED) and organic photovoltaic energy (OVP) [30,31]. The electronic and photonic properties of these type of molecules behaving as DA system are a function of the HOMO-LUMO energy [32]. Some of them have the potential as new optical materials, due to their delayed photoluminescence (DLP) behavior [33]. They may have solvatochromic effects [34,35], in addition to their importance for the detection of diseases [36].

Due to the biological importance and the multiple applications in different areas of phthalimides, isoindolin-1-ones and isoindolines including their interesting chemical and photophysical properties, in connection with our current research interest in the synthesis of 2,3-disubstituted isoindolin-1-ones [37,38], herein we describe the synthesis of three phthalimides, three isoindolin-1-ones and three isoindolines

* Corresponding author.

E-mail address: palacios@uaem.mx (M. Ordóñez).

<https://doi.org/10.1016/j.jphotochem.2021.113185>

Received 2 June 2020; Received in revised form 6 January 2021; Accepted 1 February 2021

Available online 20 March 2021

1010-6030/© 2021 Elsevier B.V. All rights reserved.

incorporating fragments of aminobenzoic acid under mild reaction conditions as well as the evaluation of their photophysical properties as donor-acceptor compounds and the correlation with their theoretical predictions.

2. Experimental section

2.1. Materials and instruments

All commercial materials were used as received noted otherwise. Reactions were monitored using analytical TLC plates (Merk, silica gel F254, 0.25 mm). Flash chromatography was performed using 230–400 mesh Silica Flash 60® silica gel. ^1H and ^{13}C spectra were recorded on a Bruker Avance DPX 200 and DPX 400 instrument operating at 400 MHz (^1H) and 100 MHz (^{13}C). Chemical shifts are reported in ppm using TMS as internal standard. Mass spectra were obtained on a Shimadzu GCMS-QP5050 instrument. Melting Points were determined on a Büchi instrument and are uncorrected. Fluorescence emission spectra were obtained using a Varian spectrofluorometer. UV–vis absorption spectra were obtained using a Cary 300 spectrophotometer.

2.2. Synthesis section

2.2.1. General procedure for the preparation of phthalimides **1a-c**

To a stirred solution of phthalic anhydride (0.25 g, 1.7 mmol) and the appropriate methyl aminobenzoate (0.26 g, 1.7 mmol) in toluene 15 mL, triethylamine (0.17 g, 1.7 mmol) was added. The reaction mixture was heated at reflux with azeotropic removal of water assisted by Dean-Stark trap. Upon completion of the reaction (12 h), it was allowed to room temperature and the formation of a solid was observed, the solvent was decanted, and the crude product was purified by column chromatography using a mixture of $\text{CH}_2\text{Cl}_2/\text{AcOEt}$ (85:15) as eluent. The ^1H and ^{13}C NMR spectroscopic data for the compounds **1a-c** are identical with those described in the literature [39].

2.2.2. General procedure for the preparation of isoindolin-1-ones **3a-c**

A solution of 2-formylbenzoic acid (0.25 g, 1.7 mmol) and phenylboronic acid (20 mg, 0.16 mmol) in methanol (5 mL) was cooled at 0°C and the appropriate methyl aminobenzoate (0.25 g, 1.7 mmol) was added. The reaction mixture was stirred at 0°C for 15 min, followed by the addition of sodium borohydride (0.75 g, 1.9 mmol). After the gas evolution was ceased, the reaction mixture was heated at 50°C for 2.0 h. After this time, the solvent was evaporated under reduced pressure and the residue was treated with aqueous solution of NH_4Cl (2 mL) and extracted with AcOEt (3×10 mL). The combined extracts were washed with brine (5 mL), dried over anhydrous Na_2SO_4 , filtered and evaporated. The residue was purified by column chromatography to obtain the corresponding isoindolin-1-ones **3a-c**. The ^1H and ^{13}C NMR spectroscopic data for the compound **3c** are identical with those described in the literature [40].

2.2.2.1. 2-(2-Methoxycarbonylphenyl)isoindolin-1-one 3a. The crude was purified by column chromatography using a mixture of $\text{CH}_2\text{Cl}_2/\text{AcOEt}$ (95:5) as eluent, obtaining (0.43 g, 95 %) of **3a** as white crystals, m.p. 151–152 $^\circ\text{C}$. ^1H NMR (400 MHz, CDCl_3): δ = 3.86 (s, 3H, CH_3O), 4.93 (s, 2H, CH_2), 6.54 (dd, J = 8.54, 1.03 Hz, 1H, H_{arom}), 6.59 (ddd, J = 8.09, 7.08, 1.07 Hz, 1H, H_{arom}), 7.26 (ddd, J = 8.68, 7.03, 1.72 Hz, 1H, H_{arom}), 7.36 (ddd, J = 7.80, 7.01, 1.64 Hz, 1H, H_{arom}), 7.48–7.52 (m, 1H, H_{arom}), 7.54 (dd, J = 7.79, 1.04 Hz, 1H, H_{arom}), 7.93 (dd, J = 8.04, 1.69 Hz, 1H, H_{arom}), 8.15 (dd, J = 7.77, 1.39 Hz, 1H, H_{arom}). ^{13}C NMR (100 MHz, CDCl_3): δ = 45.8, 51.7, 110.5, 111.9, 115.1, 127.2, 127.6, 128.2, 131.8, 132.3, 133.6, 134.7, 142.3, 151.1, 169.3, 172.8. HRMS (FAB $^+$): calculated for $\text{C}_{16}\text{H}_{13}\text{NO}_3$ [M+H] $^+$, m/z 267.0895; found for [M+H] $^+$, m/z 268.0755.

2.2.2.2. 2-(3-Methoxycarbonylphenyl)isoindolin-1-one 3b. The crude was purified by column chromatography using a mixture of $\text{CH}_2\text{Cl}_2/\text{AcOEt}$ (80:20) as eluent, obtaining (0.38 g, 85 %) of **2b** as white crystals, m.p. 123–125 $^\circ\text{C}$. ^1H NMR (400 MHz, CDCl_3): δ = 3.94 (s, 3H, CH_3O), 4.91 (s, 2H, CH_2), 7.48–7.54 (m, 3H, H_{arom}), 7.61 (ddd, 7.36, 1.07 Hz, 1H, 7.84 (d, J = 7.87, 1H, H_{arom}), 7.92 (dd, 7.56, 1.12 Hz, 1H, H_{arom}), 8.25–8.29 (m, 1H, H_{arom}), 8.37–8.41 (m, 1H, H_{arom}). ^{13}C NMR (100 MHz, CDCl_3): δ = 50.8, 52.4, 119.6, 122.9, 124.1, 124.4, 125.5, 128.6, 129.5, 131.1, 132.5, 133.1, 139.9, 140.2, 166.9, 167.8. HRMS (FAB $^+$): calculated for $\text{C}_{16}\text{H}_{13}\text{NO}_3$ [M+H] $^+$, m/z 267.0895; found for [M+H] $^+$, m/z 268.0831.

2.2.3. General procedure for the preparation of isoindolines **5a-c**

To a stirred solution of α,α' -dibromo-*o*-xyleno (0.25 g, 0.94 mmol) in acetonitrile (5 mL), K_2CO_3 (0.23 g, 2.1 mmol) and the appropriate methyl aminobenzoate (0.14 g, 0.94 mmol) was added. The reaction mixture was heated at 50°C for 3.0 h. After this time, the reaction mixture was filtered and the solid was washed with CH_2Cl_2 . The combined organic solvent was evaporated and the residue was purified by column chromatography using a mixture of $\text{CH}_2\text{Cl}_2/\text{hexane}$ (85:15) as eluent.

2.2.3.1. 2-(2-Methoxycarbonylphenyl)isoindoline 5a. White crystals (0.17 g, 69 %); m.p. 150–151 $^\circ\text{C}$. ^1H NMR (400 MHz, CDCl_3): δ = 3.84 (s, 4H, CH_2), 4.50 (s, 3H, CH_3O), 6.61 (dd, J = 8.03 Hz, 1H, H_{arom}), 6.65 (d, J = 8.53 Hz, 2H, H_{arom}), 7.24–7.27 (m, 1H, H_{arom}), 7.29–7.34 (m, 2H, H_{arom}), 7.38–7.41 (m, 1H, H_{arom}), 7.92 (dd, J = 7.99, 1.50 Hz, 1H, H_{arom}). ^{13}C NMR (100 MHz, CDCl_3): δ = 44.8, 51.7, 110.5, 111.9, 115.2, 127.9, 128.6, 131.8, 134.8, 136.3, 150.8, 169.2. HRMS (FAB $^+$): calculated for $\text{C}_{16}\text{H}_{15}\text{NO}_2$ [M+H] $^+$, m/z 253.1103; found for [M+H] $^+$, m/z 253.1024.

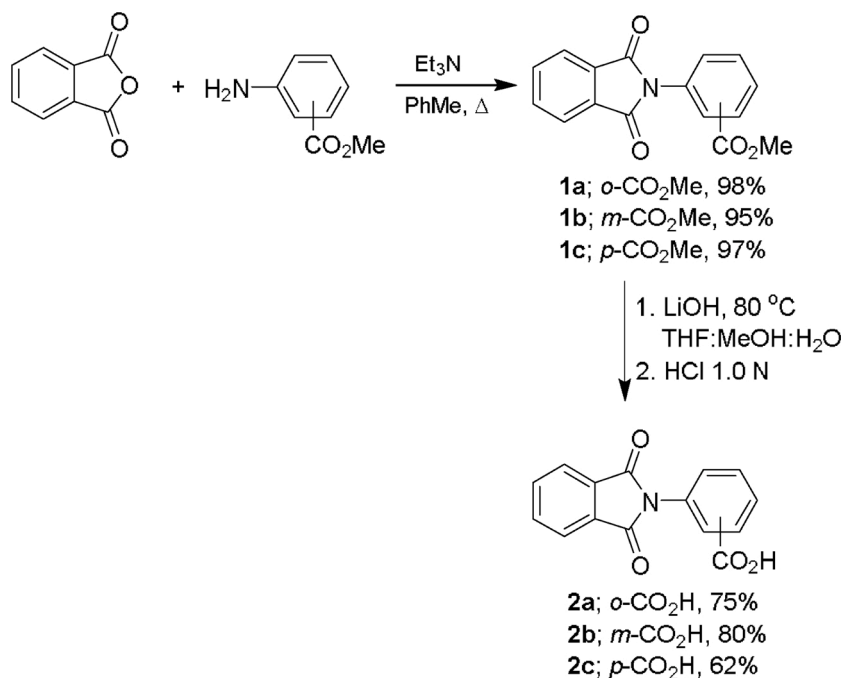
2.2.3.2. 2-(3-Methoxycarbonylphenyl)isoindoline 5b. White solid (0.20 g, 85 %); m.p. 123–123.5 $^\circ\text{C}$. ^1H NMR (200 MHz, CDCl_3): δ = 3.90 (s, 3H, CH_3O), 4.58 (s, 4H, CH_2), 6.72–6.79 (m, 1H, H_{arom}), 7.20–7.42 (m, 7H, H_{arom}). ^{13}C NMR (100 MHz, CDCl_3): δ = 52.0, 53.7, 112.3, 115.8, 117.2, 122.6, 127.2, 129.2, 130.9, 137.5, 146.9, 167.6. HRMS (FAB $^+$): calculated for $\text{C}_{16}\text{H}_{15}\text{NO}_2$ [M+H] $^+$, m/z 253.1103; found for [M+H] $^+$, m/z 253.1176.

2.2.3.3. 2-(4-Methoxycarbonylphenyl)isoindoline 5c. White solid (0.17 g, 70 %); m.p. 217–219 $^\circ\text{C}$. ^1H NMR (200 MHz, CDCl_3): δ = 3.85 (s, 3H, CH_3O), 4.67 (s, 4H, CH_2), 6.61 (system AA'BB', J = 8.97 Hz, 2H, H_{arom}), 7.29–7.35 (m, 4H, H_{arom}), 7.97 (system AA'BB', J = 8.99 Hz, 2H, H_{arom}). ^{13}C NMR (100 MHz, CDCl_3): δ = 51.6, 53.8, 110.9, 117.5, 122.8, 127.6, 131.7, 137.2, 150.3, 167.6. HRMS (FAB $^+$): calculated for $\text{C}_{16}\text{H}_{11}\text{NO}_3$ [M+H] $^+$, m/z 253.0739; found for [M+H] $^+$, m/z 253.0840.

2.2.4. General procedure for the preparation of **2a-c**, **4a-c** and **6a-c**

A solution of phthalimides **1a-c** (0.25 g, 0.88 mmol) and isoindolin-1-ones **3a-c** (0.25 g, 0.93 mmol) in a mixture of THF/MeOH/ H_2O (3:2:2) (5 mL), LiOH (0.89 g, 3.71 mmol) was added. The reaction mixture was heated at 50°C for 1.0 h. After this time, the solvent was evaporated and the resulting residue was treated with 1.0 N HCl (2 mL). The precipitated was filtered, dried and recrystallized from $\text{CH}_2\text{Cl}_2/\text{MeOH}$, obtaining the desired compounds **2a-c** and **4a-c**. The saponification of the isoindolines **5a-c** (0.25 g, 0.98 mmol) was carried out using NaOH (0.16 g, 3.92 mmol) under similar procedure, to give the isoindolines derivatives **6a-c**. The ^1H and ^{13}C NMR spectroscopic data for the compounds **2a, c** [41], **4c** [42] are identical with those described in the literature.

2.2.4.1. 2-(3-Carboxyphenyl)phthalimide 2b. White crystals (0.19 g, 80 %); m.p. 289–290 $^\circ\text{C}$. ^1H NMR (400 MHz, CDCl_3): δ = 7.46 (dd, J = 7.92 Hz, 1H, H_{arom}), 7.56–7.61 (m, 2H, H_{arom}), 7.68 (ddd, J = 7.48, 1.36 Hz, 1H, H_{arom}), 7.80 (d, J = 7.77 Hz, 1H, H_{arom}), 7.91 (ddd,



Scheme 1. Synthesis of phthalimides 2a-c.

$J = 8.14, 1.11$ Hz, 1H, H_{arom}), 8.04 (dd, $J = 7.80, 1.25$ Hz, 1H, H_{arom}), 8.31–8.32 (m, 1H, H_{arom}). ¹³C NMR (100 MHz, CDCl₃): $\delta = 113.9, 117.1, 117.6, 119.9, 121.0, 121.8, 122.6, 124.5, 131.5, 160.6, 162.4$. HRMS (FAB⁺): calculated for C₁₅H₉NO₄ [M+H]⁺, m/z 267.0532; found for [M+H]⁺, m/z 267.0498.

2.2.4.2. 2-(2-Carboxyphenyl)isoindolin-1-one 4a. White solid (0.22 g, 95 %); m.p. 176–177 °C. ¹H NMR (400 MHz, CDCl₃): $\delta = 4.85$ (s, 2H, CH₂), 6.50–6.64 (m, 2H, CH₂), 7.20–7.37 (m, 2H, H_{arom}), 7.39–7.54 (m, 2H, H_{arom}), 7.95 (dd, $J = 8.24, 1.72$ Hz, 1H, H_{arom}), 8.02 (ddd, $J = 7.37, 1.32, 0.63$ Hz, 1H, H_{arom}). ¹³C NMR (100 MHz, CDCl₃): $\delta = 45.4, 110.2, 111.6, 112.2, 114.7, 126.9, 128.2, 129.2, 131.4, 132.4, 134.6, 141.1, 151.2, 169.9, 171.2$. HRMS (FAB⁺): calculated for C₁₅H₁₁NO₃ [M+H]⁺, m/z 253.0739; found for [M+H]⁺, m/z 253.0730.

2.2.4.3. 2-(3-Carboxyphenyl)isoindolin-1-one 4b. White crystals (0.20 g, 86 %); m.p. 235–270 °C. ¹H NMR (400 MHz, CDCl₃): $\delta = 5.11$ (s, 2H, CH₂), 7.52–7.63 (m, 2H, CH₂), 7.67–7.84 (m, 4H, H_{arom}), 8.21 (d, $J = 8.0$ Hz, 1H, H_{arom}), 8.54 (s, 1H, H_{arom}). RMN ¹³C (100 MHz, CDCl₃): $\delta = 50.8, 120.2, 123.6, 123.7, 123.8, 125.1, 128.6, 129.7, 131.9, 132.6, 132.9, 140.1, 141.5, 167.3, 167.5$. HRMS (FAB⁺): calculated for C₁₅H₁₁NO₃ [M+H]⁺, m/z 253.0739; found for [M+H]⁺, m/z 253.0744.

2.2.4.4. 2-(2-Carboxyphenyl)isoindoline 6a. Colorless oil (0.17 g, 70 %). ¹H NMR (400 MHz, CDCl₃): $\delta = 5.48$ (s, 4H, CH₂), 6.52–6.67 (m, 1H, H_{arom}), 7.19–7.30 (m, 2H, H_{arom}), 7.34–7.43 (m, 2H, H_{arom}), 7.48–7.55 (m, 2H, H_{arom}), 7.87 (d, $J = 8.03$ Hz, 1H, H_{arom}). ¹³C NMR (100 MHz, CDCl₃): $\delta = 63.8, 110.6, 116.4, 116.8, 128.8, 129.9, 131.4, 134.4, 135.0, 150.8, 167.8$. HRMS (FAB⁺): calculated for C₁₅H₁₃NO₂ [M+H]⁺, m/z 239.0946; found for [M+H]⁺, m/z 239.0932.

2.2.4.5. 2-(3-Carboxyphenyl)isoindoline 6b. Yellow solid (0.18 g, 78 %); m.p. 176–178 °C. ¹H NMR (400 MHz, CDCl₃): $\delta = 4.64$ (s, 4H, CH₂), 6.87 (d, $J = 7.55$ Hz, 1H, CH₂), 7.28–7.33 (m, 4H, H_{arom}), 7.36 (d, $J = 7.83$ Hz, 1H, H_{arom}), 7.39–7.42 (m, 2H, H_{arom}). ¹³C NMR (100 MHz, CDCl₃): $\delta = 53.8, 112.5, 116.4, 117.3, 123.2, 127.7, 129.8, 132.1, 137.9, 147.4, 168.4$. HRMS (FAB⁺): calculated for C₁₅H₁₃NO₂ [M+H]⁺, m/z 239.0946; found for [M+H]⁺, m/z 239.0902.

2.2.4.6. 2-(4-Carboxyphenyl)isoindoline 6c. White solid (0.15 g, 62 %); m.p. 204–206 °C. ¹H NMR (400 MHz, CDCl₃): $\delta = 4.69$ (s, 4H, CH₂), 6.70 (system A'ABB', $J = 8.54$ Hz, 2H, H_{arom}), 7.32–7.34 (m, 2H, H_{arom}), 7.40–7.43 (m, 2H, H_{arom}), 7.84 (system A'ABB', $J = 8.57$ Hz, 2H, H_{arom}). ¹³C NMR (100 MHz, CDCl₃): $\delta = 53.7, 111.4, 118.0, 123.2, 127.8, 131.7, 137.5, 150.4, 168.1$. HRMS (FAB⁺): calculated for C₁₅H₁₃NO₂ [M+H]⁺, m/z 239.0946; found for [M+H]⁺, m/z 239.0963.

2.3. Quantum yield calculation

The quantum yields (ϕ_F) were determined following the Eq. 1.

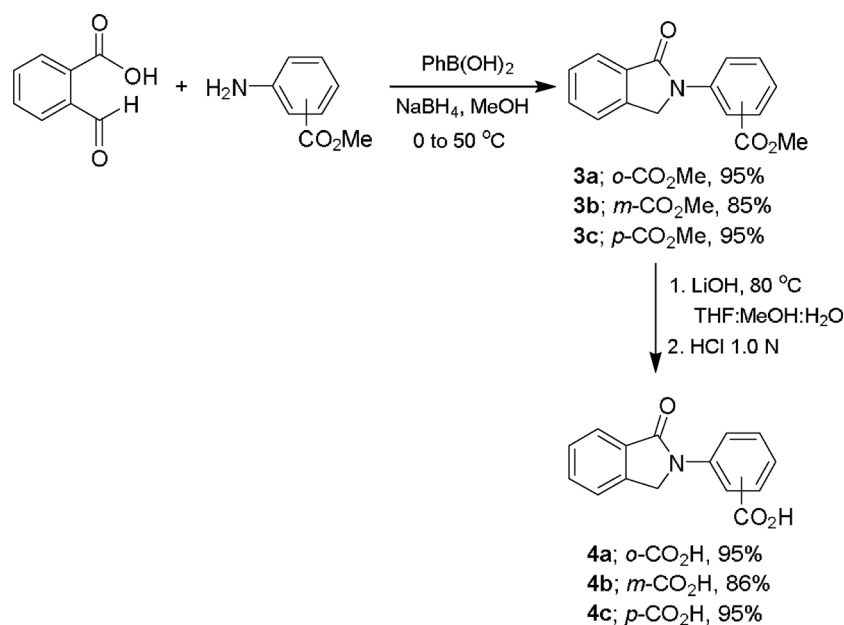
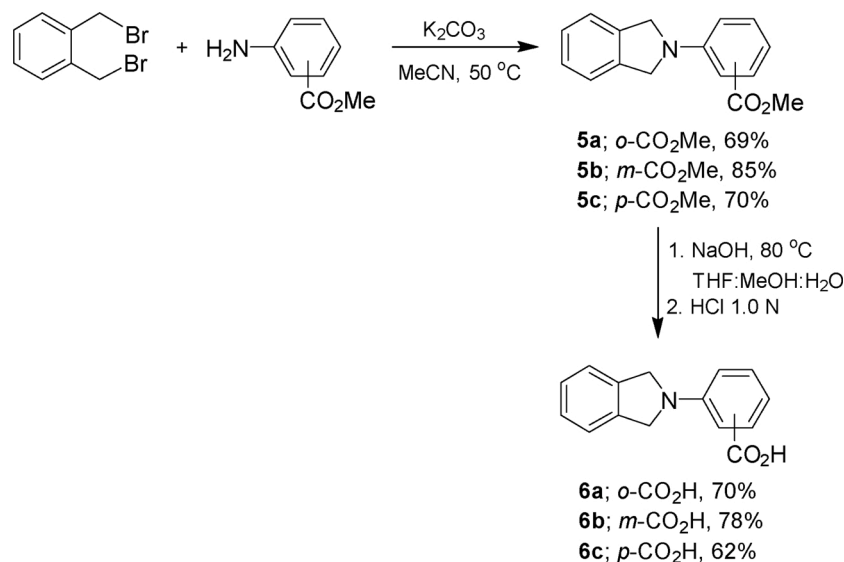
$$\phi_F = \phi_R \times \frac{\text{Int } A_R n^2}{\text{Int } A n^2_R} \quad (1)$$

Where ϕ_F is the sample quantum yield, *Int* is the area under the emission peak (at a given wavelength scale), *A* is the absorbance at the excitation wavelength, and *n* is the refractive index of the sample. The subscript *R* denotes the respective values of the reference substance. The reference substance was anthracene.

Fluorescence quantum yield was calculated by preparing ten anthracene samples in ethanol used as standard. The nine compounds were dissolved in methanol, found that the samples present absorbances between 0.01–0.1. The fluorescence spectra of the same samples were obtained with a slit 2.5:2.5 and the integral of the fluorescence intensity (that is, the area of the fluorescence spectrum) was calculated. Finally, the magnitude of the integrated fluorescence intensity was plotted against the obtained absorbance. The result is a straight line with gradient proportional to the quantum yield. The absolute values were calculated using standard samples (anthracene) that have fixed with fluorescence quantum yield reported.

2.4. Free energy calculations

All the calculations described were performed with the GAUSSIAN 09 quantum chemistry package [43]. The ground and excited states geometries of the nine compounds have been optimized at PCM/B3LYP/TDDFT/6–311++G(d,p) level of theory. We have used the popular B3LYP hybrid functional in all cases, which mixes the Lee, Yang and Parr functional for the correlation part and Becke's three-parameter

Scheme 2. Synthesis of *N*-substituted isoindolin-1-ones 4a-c.

Scheme 3. Synthesis of isoindolines 6a-c.

functional for the exchange [44,45]. The geometry optimization was performed in methanol using 6-311++G(d,p) basis set. The influence of solvent (methanol) was simulated within the integral-equation-formalism version of the polarizable continuum model (IEFPCM) developed by Tomasi et al. [46,47]. The wavelengths corresponding to vertical transitions from S_0 to a singlet excited state S_1 , and oscillator strengths of each S_0 - S_1 were calculated.

3. Results and discussion

3.1. Design and preparation

For the synthesis of the target phthalimides **2a-c**, initially we carried out the condensation of phthalic anhydride with the corresponding methyl aminobenzoates in the presence of Et₃N in toluene at reflux under azeotropic removal of water [48], obtaining the phthalimides **1a-c** in excellent yields, which by saponification with LiOH in a mixture

of THF:MeOH:H₂O at 80 °C, followed by the treatment with 1.0 N HCl, afforded the phthalimides **2a-c** in 62–80% yield (Scheme 1).

On the other hand, for the synthesis of the target *N*-substituted isoindolin-1-ones **4a-c**, the 2-formylbenzoic acid was reacted with the appropriate methyl aminobenzoates in the presence of catalytic amounts of phenylboronic acid as catalyst [20,49] in methanol at 0 °C, followed by the addition of NaBH₄ and subsequent heating at 80 °C for 3.0 h, to obtain the isoindolin-1-ones derivatives **3a-c** in 85–95% yield. Saponification of methyl ester in **3a-c** with LiOH in a mixture of THF:MeOH:H₂O at 80 °C and subsequent treatment with 1.0 N HCl, afforded the *N*-substituted isoindolin-1-ones **4a-c** in 86–95% yield (Scheme 2).

Finally, for the synthesis of isoindolines **6a-c**, initially we carried out the reaction of α,α' -dibromo-*o*-xylene with the corresponding methyl aminobenzoates and K₂CO₃ in acetonitrile at 50 °C for 3.0 h, to obtain the isoindolines **5a-c** in 69–85% yield, which by saponification with NaOH in a mixture of THF:MeOH:H₂O at 80 °C and subsequent treatment with 1.0 N HCl, produced the *N*-substituted isoindolines **6a-c** in

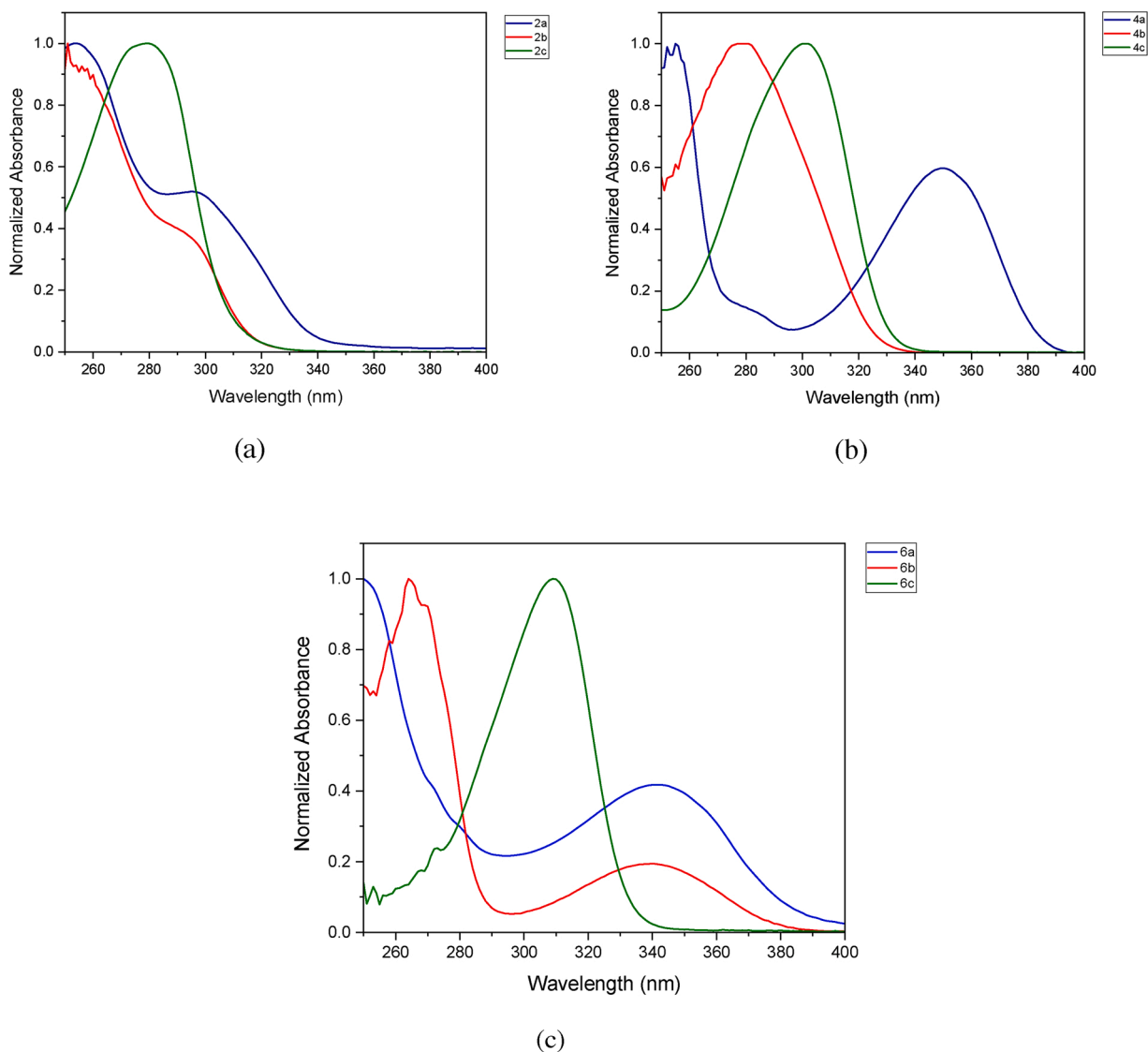


Fig. 1. Absorbance spectra for: (a) phthalimides **2**, (b) isoindolin-1-ones **4** and (c) isoindolines **6** in MeOH at 2.5×10^{-5} M.

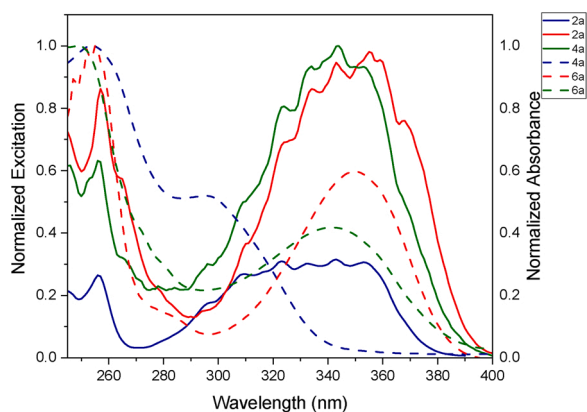


Fig. 2. Excitation (solid line) and absorbance (dashed line) spectra for phthalimide **2a**, isoindolin-1-one **4a** and isoindoline **6a** in methanol at 2.5×10^{-5} M.

62–78% yield (Scheme 3).

3.2. Spectral measurements

With the compounds **2a-c**, **4a-c** and **6a-c** in hand, we carried out the studies of electronic absorption and fluorescence emission, which were performed in methanol HPLC grade at a concentration of 2.5×10^{-5} M. These compounds exhibit strong absorption band between 275–380 nm, corresponding to $\pi\text{-}\pi^*$ and $\eta\text{-}\pi^*$ transitions of the corresponding singlet-singlet transitions (Fig. 1). The $\eta\text{-}\pi^*$ transitions are given by the delocalization of N electron pair to the carboxylic acid in the DA system. Also, it can be observed that the maximum absorbance wavelength is affected by the position of the carboxylic acid in the aromatic ring. The pattern *ortho* > *meta* > *para* is followed by phthalimides **2** and isoindolines **6**, but a sequence *ortho* > *para* > *meta* is observed in the isoindolin-1-ones **4**. As it is well known, the band position is related with the HOMO-LUMO energy involved in the transition.

The excitation spectra were acquired and compared with the absorbance spectra, where the transitions of the basal state are the same as in the excited state (Fig. 2). Highlighting the bands of minimum energy around 275–350 nm corresponding to the $\eta\text{-}\pi^*$ transitions. Bands at 250 nm were also observed, corresponding to the absorbance spectrum, which include the $\pi\text{-}\pi^*$ transitions.

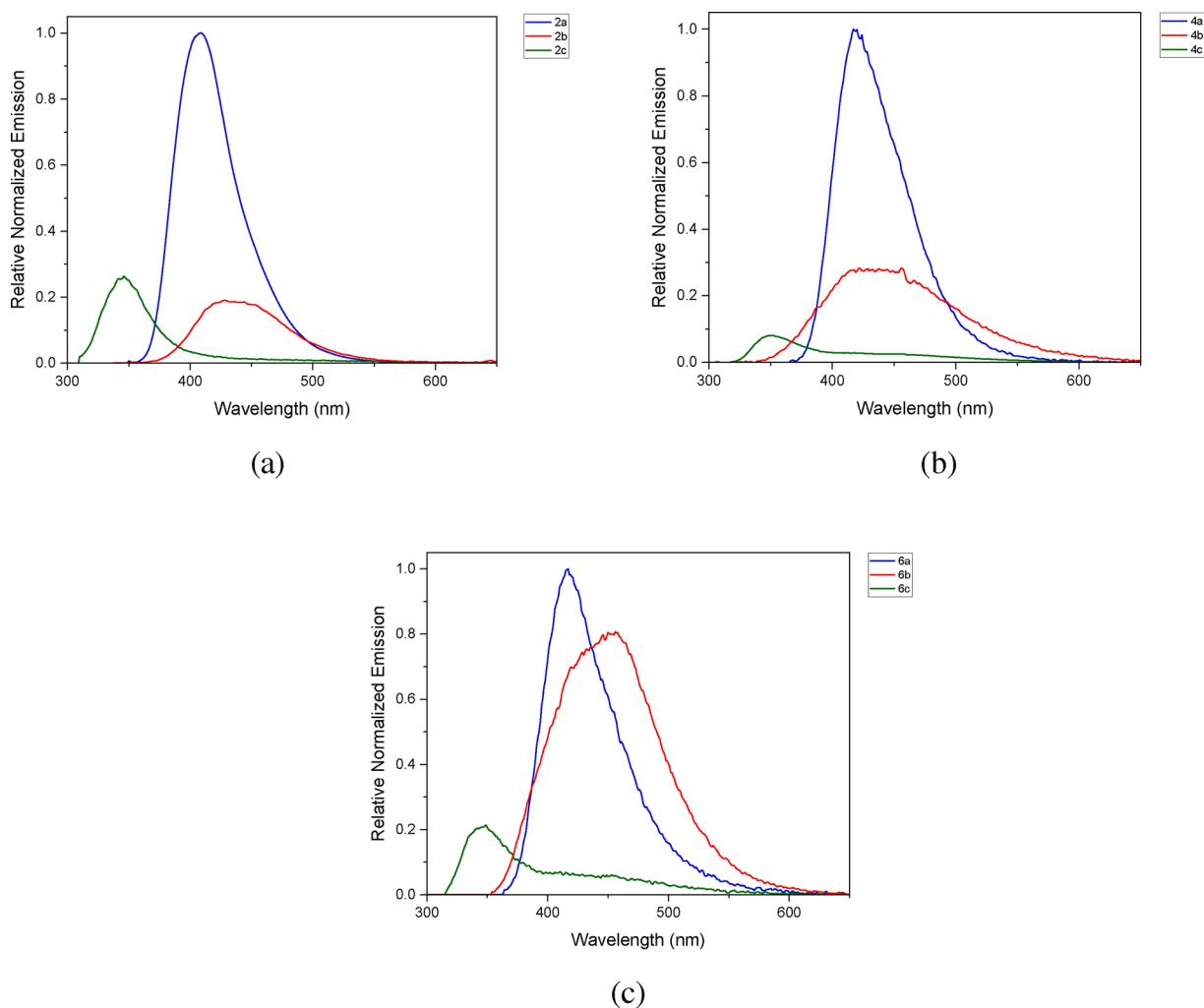


Fig. 3. Fluorescence spectra for (a) phthalimides **2**, (b) isoindolin-1-ones **4** and (c) isoindolines **6** in methanol at 1×10^{-4} M.



Fig. 4. Solutions of compounds **2**, **4** and **6** irradiated under UV light at 365 nm.

Table 1

Photophysical data for the phthalimides **2**, isoindolin-1-ones **4** and isoindolines **6**.

Compound	Photophysical data							
	λ_{abs} (nm)	λ_{em} (nm)	Φ_F	Optical gap (eV)	HOMO-LUMO s_0, s_1 (eV)	Optical gap (eV)	LUMO-HOMO s_1, s_0 (eV)	SS
2a	298	410	0.19 (± 0.04)	4.16	4.74	3.02	3.04	112
2b	292	431	0.05 (± 0.03)	4.24	4.58	2.87	3.00	139
2c	280	346	0.073 (± 0.04)	4.42	4.53	3.58	3.04	66
4a	351	422	0.56 (± 0.02)	3.53	5.41	2.93	3.42	71
4b	281	418	0.45 (± 0.02)	4.41	4.71	2.96	4.02	137
4c	303	351	0.19 (± 0.03)	4.09	4.52	3.53	3.69	48
6a	344	414	0.58 (± 0.01)	3.60	5.05	2.99	3.48	70
6b	341	459	0.508 (± 0.03)	3.63	4.01	2.70	3.41	118
6c	310	356	0.34 (± 0.04)	3.99	4.36	3.48	4.10	46

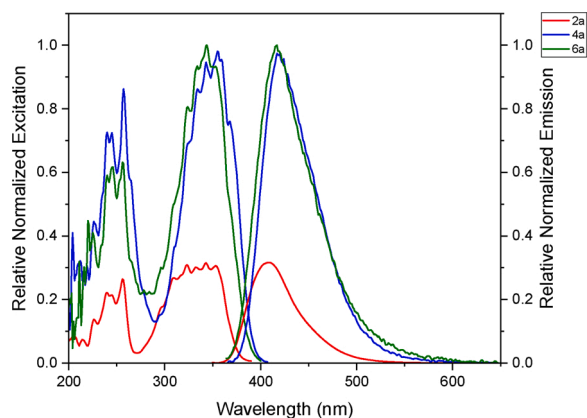


Fig. 5. Excitation and fluorescence spectra for phthalimides **2a**, isoindolin-1-one **4a** and isoindoline **6a** in methanol at 1×10^{-4} M.

Table 2
Different conformation of the molecule **4a**.

	θ	Hartree	Mol 4
a	-20.3466	-858.9214	
b	19.6534	-858.9152	
c	79.6534	-858.9248	
d	129.6532	-858.9212	
e	139.6535	-858.9268	
f	179.6532	-858.9181	
g	-90.3464	-858.9286	

The fluorescence emission for the compounds **2**, **4** and **6** in methanol at room temperature (Fig. 3) are similar to those observed in previously reported analogues [28,50,51]. The emission wavelengths obtained are between 350 and 450 nm. With an intensity trend of *ortho* > *para* > *meta* in case of phthalimides **2** and *ortho* > *meta* > *para* for the isoindolin-2-ones **4** and isoindolines **6**. For the compounds with substituents in *para* position, the emission bands were displaced to areas of greater energy. Whereas for the phthalimides **2** and isoindolines **6** with the carboxylic acid in *meta* position- the emission bands are at lower energy, and for isoindolin-1-ones **4** with the carboxylic acid in *ortho* position is most displaced to red. The isoindolin-1-one **4b**, although its emission is not so red with a band at 418 nm, has the highest Stokes shift (137 nm). This trend is maintained regarding the displacements for the rest of the target families *meta* > *ortho* > *para*.

Solutions of compounds **2**, **4** and **6** irradiated under UV light at 365 nm are shown in Fig. 4.

The obtained quantum yields give important information about the fluorescent properties of these compounds, such as their efficiency as fluorophores, generating information on their possible applications. Noteworthy, the number of carbonyl groups has an influence over the quantum yields (Table 1). The isoindolines **6** present the higher fluorescence quantum yields followed by isoindolin-1-ones **4**, and finally the phthalimides **2** (Fig. 5). The quantum yields of phthalimides **2** follows the *ortho* > *para* > *meta* order and for the isoindolin-1-ones **4** and isoindolines **6** is *ortho* > *meta* > *para*, which are in agreement with the fluorescence spectra presented in Fig. 3. These results may suggest a predominant electronic effect in compounds **2** and a combination of electronic and conformational in compounds **4** and **6**.

The photophysical parameters of **2**, **4** and **6** in methanol are listed in Table 1.

Some studies carried out on the indoprofen and ketoprofen show that a transition of a singlet to the triplet state is possible due to the presence of the carbonyl groups in the compounds, where are attributed to transitions $\eta-\pi^*$ [52]. The lower quantum yields in compounds **2** and **4** may be a consequence of a similar phenomenon in these compounds.

3.3. Molecular geometry optimization

To give us insight into the effect of base stacking on fluorescent properties of phthalimides **2**, isoindolin-1-ones **4** and isoindolines **6**, we used time-dependent density functional theory (TD-DFT) calculations to address the excited-state energies of all compounds. Several groups have used this method to address the spectroscopic results in Schiff bases within organic solvents [53,54].

It was possible to use connections that are not symmetrical and the mobility of the number of atoms during the optimization. The position of benzoic acid was optimized with respect to isoindolin-1-one rotating at certain angle the simple bond between the N and C atoms (Table 2). As a result of this calculation, the XYZ coordinates of the optimized lower energy structure were taken to improve the optimization of a ground state (Table 2). Once the ground state optimization of the basic state has been completed, the lower energy molecule "g" was chosen, with a dihedral angle of -90.3464 and an energy of -858.9286. The found conformer must be brought to an excited state (S_1) of the calculation, thus completing the S_0-S_1 transition, the state S_1 is again optimized to obtain the lower energy geometry, which simulates the non-luminescent relaxation of the molecule in the excited state. In this calculation the HOMO and LUMO orbitals responsible for the emission were obtained.

As can be seen in Fig. 6, the conformations of S_0 and S_1 singlet states which simulates the energy absorption process promoting to an excited state in the three *ortho* analogues (**2a**, **4a** and **6a**) keep the same symmetry with the same dihedral angle between the atoms 7, 8, 9 y 12. As already observed in the experimental analysis, the presence of carbonyls in the compound have an important role in the behavior of absorption and emission, and according to the calculations as the number or carbonyls decreases, so it does the conformational restriction, then we can

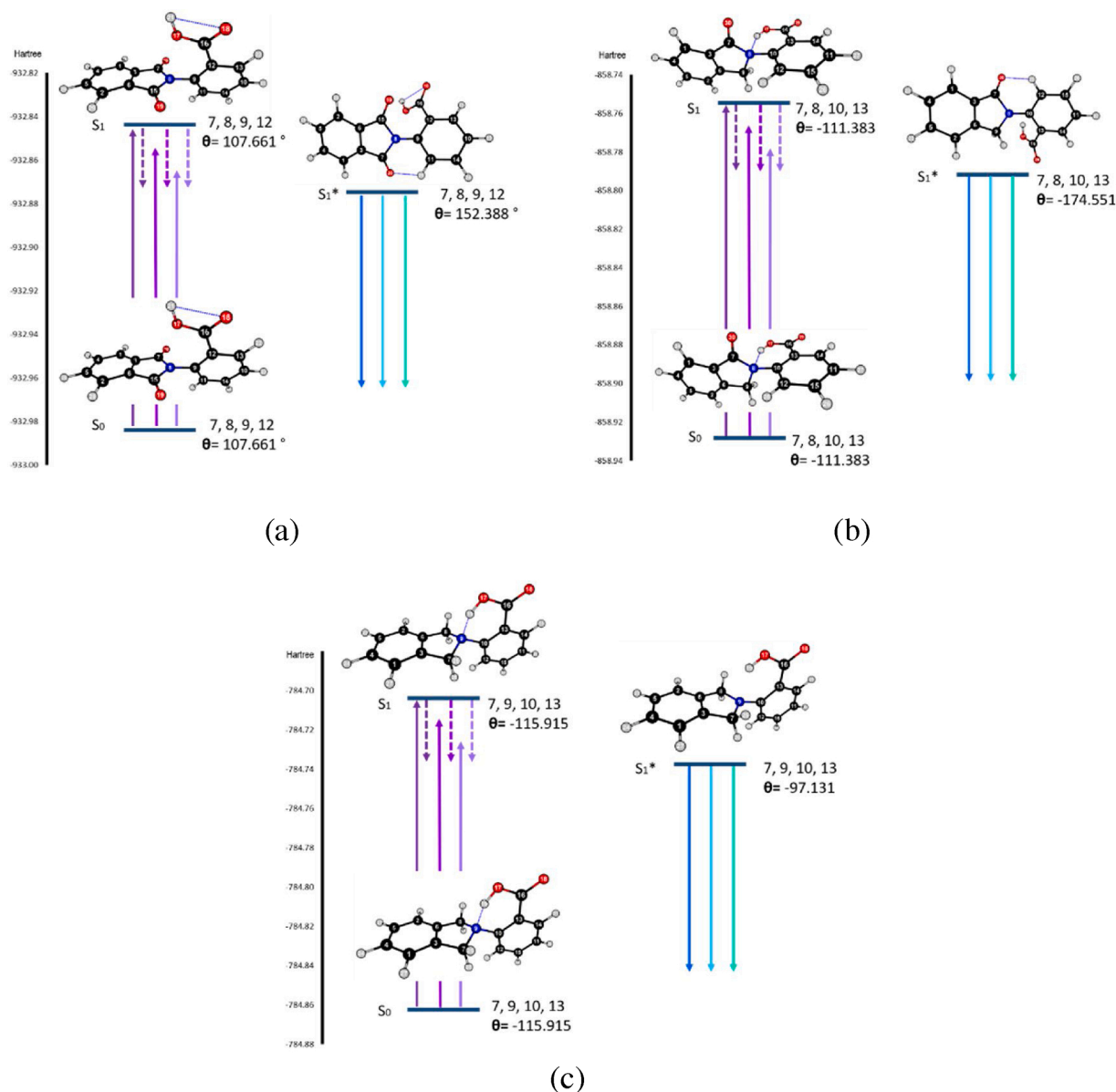


Fig. 6. Phthalimide 2a, isoindolin-1-one 4a and isoindoline 6a dihedral angles.

see a change of the dihedral angle. In addition, as we can observe that the decrease of this restriction allows an interaction between the nitrogen atom (N) of the ring with the carboxyl group, then the conformation is now mediated by a hydrogen bond in the basal state in **4a** and **6a** structures.

The following process according to the Jablonski diagram, is the molecule relaxation through non-radiative processes such as vibrational relaxation, intramolecular shocks or internal conversion. This process was simulated in the theoretical calculations and optimization of the molecule on the excited state (S_1) looking for the vibrational state of lower energy, this theoretical state is known as S_1^* . The molecule changed its dihedral angle, showing a conformation with a tendency to planarity and lower energy, at this point the molecule may emit energy as luminescence and return to the basal state.

The optimization process of states S_0 - S_1 y S_1 - S_1^* was carried out in the same way for all compounds, obtaining the molecular energies of these in different states of the luminescent process, as well as the angles and the HOMO and LUMO involved. As it can be seen in Fig. 7, phthalimides **2** need similar energies to change from HOMO to LUMO, while for isoindolin-1-ones **4** and isoindolines **6** there is a marked difference

for each of constitutional isomers of these compounds, so we can say that absorption is affected directly by the position of the carboxylic acid in the aromatic ring, being favored for the compounds substituted in *ortho* position.

In order to visualize the main contributions for the S_0 - S_1 and S_0 - S_1^* differences, the relative energies of the HOMO-LUMO orbitals are presented (Fig. 8). Most of the main contributions belong to the single HOMO-LUMO transition (the percentage for all the compounds may be consulted in the Supporting Information). In Fig. 7 it can be observed that the energy necessary for the transition in phthalimides **2** are similar, while in the isoindolin-1-one **4** and isoindolines **6** have a small difference in the transition energies. When the transitions HOMO to LUMO and LUMO to HOMO are compared, it is appreciated that the emission process energy is lower than absorption process, which indicates that calculations fit to the Stokes shift shown by experiments. Moreover, the tendency of this Stokes shift for every group is well predicted by the theory, e.g. **6c** is blue shifted, **6a** remains in the middle and **6b** is red shifted. For all the cases the S_1 explore the excited state surface towards planarity in the S_1^* .

As can be seen in Fig. 8, the electron density on the behavior of the

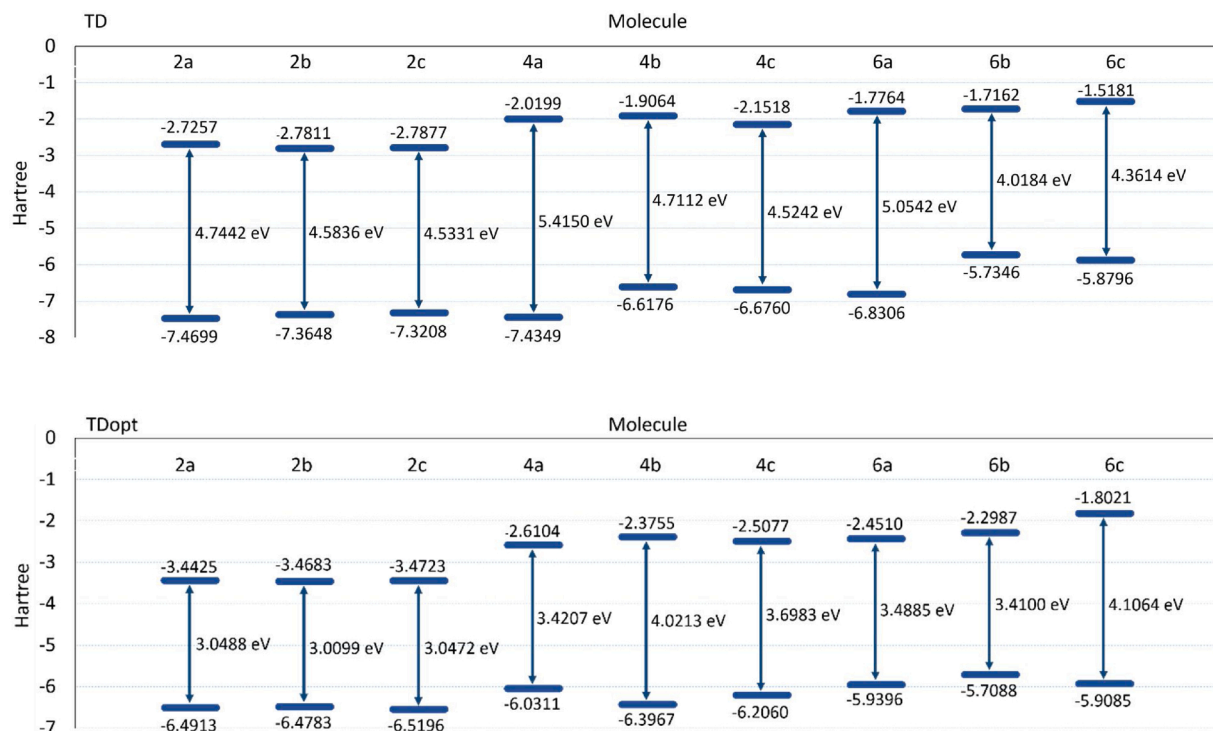


Fig. 7. HOMO-LUMO energy gap transitions of TD and TDopt phthalimides 2, isoindolin-1-ones 4 and isoindolines 6 estimated by TDDFT calculations.

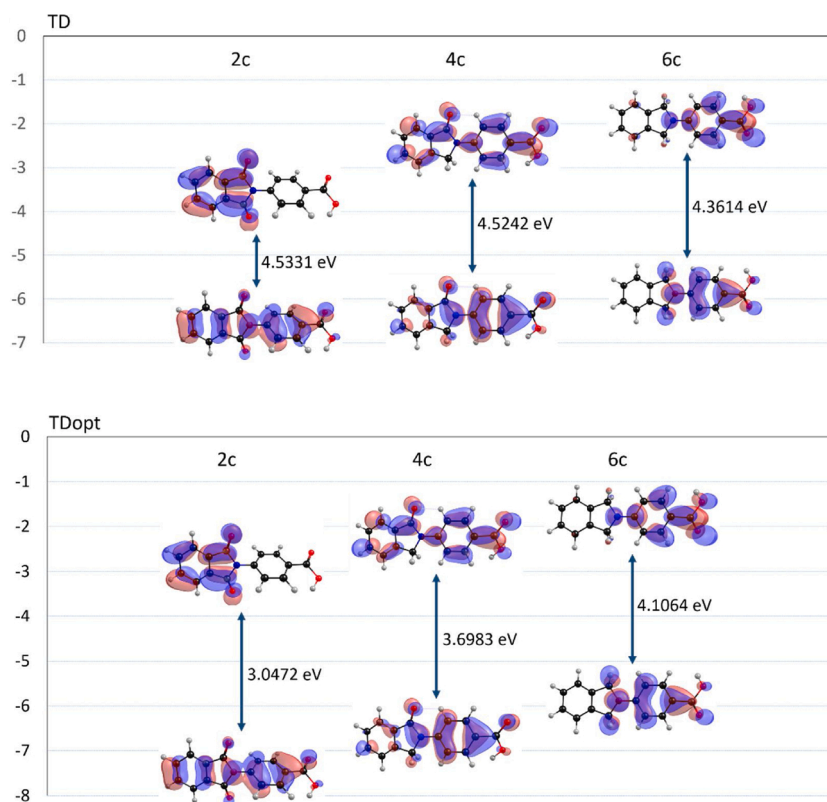


Fig. 8. Energy diagram of the orbitals HOMO-LUMO of TD and TDopt phthalimides 2, isoindolin-1-ones 4 and isoindolines 6 estimated by TDDFT calculations.

orbitals is equal to S_0-S_1 and $S_0-S_1^*$, where the electron density is the same for Fig. 8a and b. It is remarkable that the presence of O in the molecule induces a stability, so it becomes less energy as can be seen in phthalimide 2c. For isoindolin-1-one 4c it is seen how the attraction of

carboxylic acid begins to participate, so that the electron density is distributed throughout the molecule in the ground state, but at the moment of excitation this distribution moves towards the acid. Finally, in the isoindoline 6c most of the electron density is concentrated

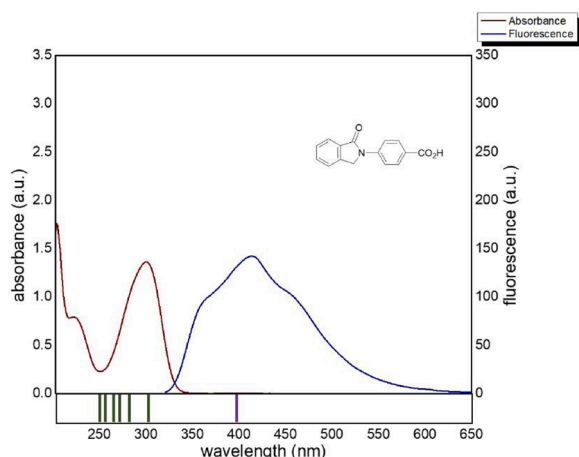


Fig. 9. Absorbance and Fluorescence spectra of isoindolin-1-one **4c** and theoretical wavelength.

towards the carboxylic acid, this tendency is observed from the HOMO state.

As mentioned above, the calculations of linear response theory, throw data on the spectrum information, for example, the wavelength where it can be seen some of the bands, and this helps us to check if the calculations are correct. In Fig. 9, it is observed the absorption and emission spectrum of the compound **4c**, in the lower part of the spectrum the signals that throw the calculations on the possible wavelengths that would appear absorption and emission bands, being evident that they are very similar.

In summary, the theoretical calculations help to understand the behavior of the compounds during the luminescence process, however,

there was still data that did not match with the experimental results, so, by doing a search in the literature, it was found that these compounds can make banned transitions, with which they would be moving from a single state to the triplet state [55,56]. For that reason, we calculated the triplet state for our nine compounds. Due to the carbonyl groups present and the known photochemistry primary processes that these groups can carry out, in particular S_1-T_n [57] this calculation give us insight into the energies of the orbitals on the triplet state, where it might be possible a change of multiplicity. El-Sayed's rules state the three major reasons a singlet-triplet intersystem crossing (ISC) may increase its probability and kinetics. As intersystem crossing is forbidden by rules of conservation of energy and angular momentum, usually its kinetics is quite slower than other photophysical processes. However, El-Sayed's rules predict an acceleration of the lowest singlet state to the triplet manifold if the ISC transition involves a change of molecular orbital type, homoenergetic S_1-T_n states, and high density of receiving states.

In the case of phthalimides, some reports [58,59] state that these compounds present triplet states formation after primary excited state formation. As presented in Fig. 10, the presence of high density of isoenergetic triplet orbitals nearby S_1 singlet state, may promote a fast transition. The presence of oxygen atom provides those energy levels that could please this need. Besides the distribution of the orbitals in the excited state seems to favor this transition and, in this way, the low yields presented by this family of compounds could be explained.

Looking in detail the isoindolin-1-one isoenergetic states in Fig. 10 calculations this level of theory predicts the existence of upper triplet states that enhance ISC. Moreover, the **4c** molecule is quite like indo profen and there are reports [27,60] where they explain the transition that this drug produces triplet states upon excitation. We can say that the quantum yields of these compounds are low because some of them convert into triplet states. For isoindolines **6a-c**, the absence of carbonyls favors fluorescence, although these compounds do not have

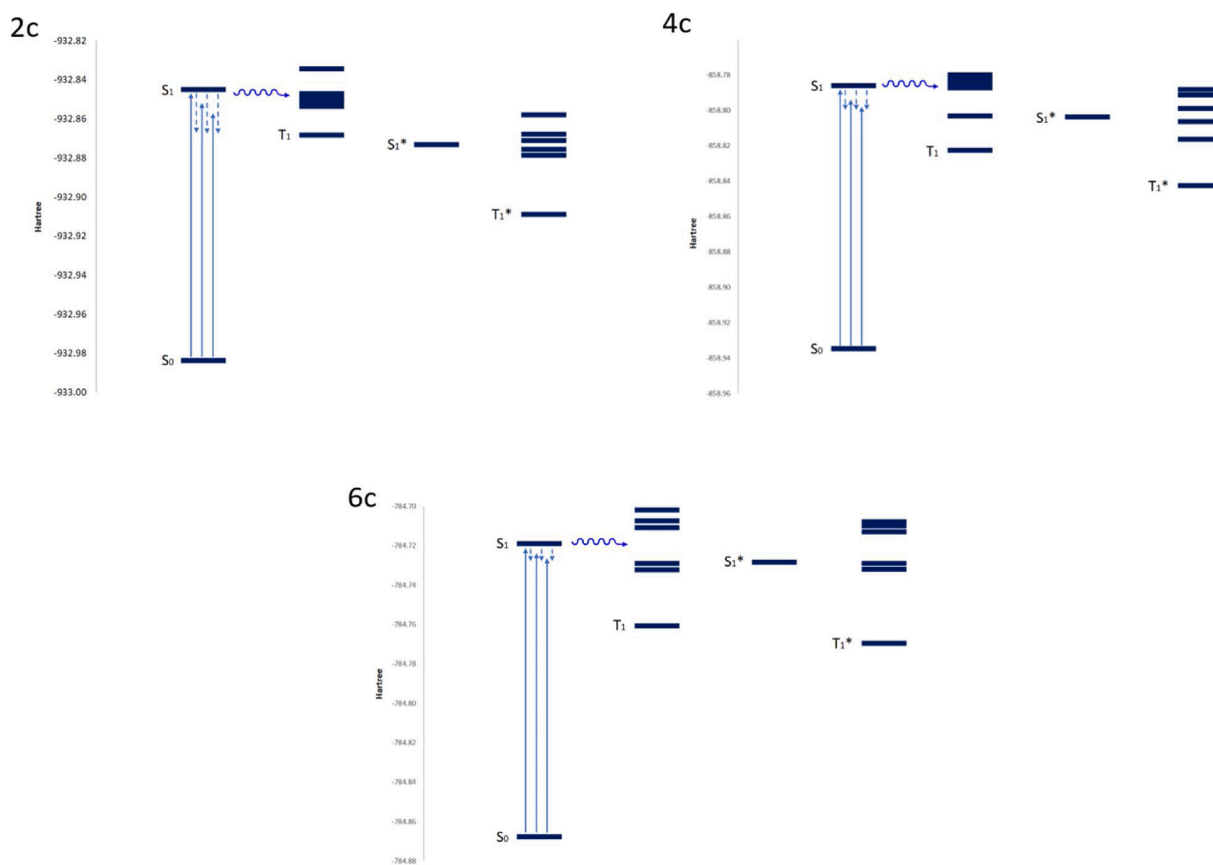


Fig. 10. Energy diagram of phthalimide **2c**, isoindolin-1-one **4c** and isoindoline **6c** S_0 - S_1 , S_0 - S_1^* and S_1 - T_1 .

strong conjugation and rigidity like phthalimides **2** and isoindolin-1-ones **4**, the availability to delocalize the electrons of nitrogen is favored, and thus the fluorescence is improved in these compounds.

4. Conclusions

Nine new fluorescent compounds were obtained in excellent yields under mild, efficient and simple processes. According to the results of the fluorescence study, the compounds behave like a donor-acceptor system, identifying the electronic transitions of the fluorescence; it also shown that the presence of carbonyl group in the compound plays an important role in the emission, directly affecting the quantum yields. In that way, the absence of carbonyls allows a better electronic delocalization and conjugation improving the luminescence. On the other hand, the *ortho* position of the carboxylic acid in the aromatic ring enhances the fluorescence, as *ortho* isoindolin-1-one **4a** presents the best quantum yield and intensity for all species. Theoretical calculations fit well to experimental results; thus, the position of the carboxylic acid affects the dihedral angle generating a rigidity that favors the transitions of the compounds to the excited states. In some compounds red shifted emission is presented, calculations confirm the almost same energy singlet-triplet states probably indicating triplet population presence and phosphorescence. Besides the biological and industrial importance of these compounds, their intrinsic fluorescence may be useful as biological probes. Furthermore, the dual luminescence is a desirable property as additional spectroscopic features (increased time and bandwidth) and this behavior is not usual in such small molecules. Hence further research on the origin and the environmental conditions that influence in this optical phenomenon is required in this kind of compounds.

Author statement

The work in this manuscript was developed in the Universidad Autónoma del Estado de Morelos (UAEM) and funded by the Consejo Nacional de Ciencia y Tecnología (CONACYT) of México via project 286614. The authors declare that they have no conflict of interest between themselves, and that they have no conflict with the University of Morelos (UAEM) or with CONACYT in order to publish the results of their investigation in the Journal of Photochemistry & Photobiology, A: Chemistry

Declaration of Competing Interest

The authors declare no conflict of interest.

Acknowledgements

The authors thank the CONACYT of Mexico, for their financial support via project 286614. M. S. S. also wishes to thank CONACYT for Graduate Scholarships 388503.

Appendix A. Supplementary data

Supplementary material related to this article can be found, in the online version, at doi:<https://doi.org/10.1016/j.jphotochem.2021.113185>.

References

- [1] B. Valeur, M.N. Berberan-Santos, *Molecular Fluorescence: Principles and Applications*, Wiley-VCH Weinheim, Germany, 2012.
- [2] B. Wang, E.V. Anslyn, *Chemosensors: Principles, Strategies and Applications*, Wiley, New Jersey, 2011.
- [3] A.D. Johnson, R.M. Curtis, K.J. Wallace, Low molecular weight fluorescent probes (LMFPs) to detect the group 12 metal triad, *Chemosensors* 7 (2019) 22.

- [4] S. Lohar, K. Dhara, P. Roy, S.P.S. Babu, P. Chattopadhyay, Highly sensitive ratiometric chemosensor and biomarker for cyanide ions in the aqueous medium, *ACS Omega* 3 (2018) 10145–10153.
- [5] D. Wu, A.C. Sedgwick, T. Gunnlaugsson, E.U. Akkaya, J. Yoon, T.D. James, Fluorescent chemosensors: the past, present and future, *Chem. Soc. Rev.* 46 (2017) 7105–7123.
- [6] Y.-C. Cai, C. Li, Q.-H. Song, Fluorescent chemosensors with varying degrees of intramolecular charge transfer for detection of a nerve agent mimic in solutions and in vapor, *ACS Sens.* 26 (2017) 834–841.
- [7] A. Reiffers, C. Torres Ziegenbein, L. Schubert, J. Diekmann, K.F. Thom, R. Kühnemuth, A. Griesbeck, O. Weingart, P. Gilch, On the large apparent Stokes shift of phthalimides, *Phys. Chem. Chem. Phys.* 21 (2019) 4839–4853.
- [8] A. Fernandez-Vidal, L.C. Arnaud, M. Maumus, M. Chevalier, G. Mirey, B. Salles, J. Vignard, E. Boutet-Robinet, exposure to the fungicide captan induces DNA base alterations and replicative stress in mammalian cells, *Environ. Mol. Mutagen.* 60 (2018) 286–297.
- [9] S. Pitschiaya, L.A. Heinicke, T.C. Custer, N.G. Walter, Single molecule fluorescence approaches shed light on intracellular RNAs, *Chem. Rev.* 114 (2014) 3224–3265.
- [10] W.-W. Zang, W.-L. Mao, Y.-X. Hu, Z.-Q. Tian, Z.-L. Wang, Q.-J. Meng, Phenothiazine-anthraquinone donor-acceptor molecules: synthesis, electronic properties and DFT-TDDFT computational study, *J. Phys. Chem. A* 113 (2009) 9997–10004.
- [11] M. Chapran, R. Lytvyn, C. Begel, G. Wiosna-Salyga, J. Ulanski, M. Vasylieva, D. Volyniuk, P. Data, J.V. Grazulevicius, High-triplet-level phthalimide based acceptors for exciplexes with multicolor emission, *Dye. Pigment.* 162 (2019) 872–882.
- [12] F. Durmur, M. Ibrahim-Ouali, D. Gimes, Organic light-emitting diodes based on phthalimide derivatives: improvement of the electroluminescence properties, *App. Sci.* 8 (2018) 539–548.
- [13] A.P. Kulkarni, Y. Zhu, A. Babel, P.-T. Wu, S.A. Jenekhe, New ambipolar organic semiconductors. 2. Effects of Electron acceptor strength on intramolecular charge transfer photophysics, highly efficient electroluminescence, and field-effect charge transport of phenoxazine-based donor-acceptor materials, *Chem. Mater.* 20 (2008) 4212–4223.
- [14] M.M. Richter, Electrochemiluminescence (ECL), *Chem. Rev.* 104 (2004) 3003–3036.
- [15] X. Sun, Y. Liu, X. Xu, C. Yang, G. Yu, S. Chen, Z. Zhao, W. Qiu, Y. Li, D. Zhu, Novel electroactive and photoactive molecular materials based on conjugated donor-acceptor structures for optoelectronic device applications, *J. Phys. Chem. B* 109 (2005) 10786–10792.
- [16] Y. Suzuki, K. Yokoyama, Development of functional fluorescent molecular probes for the detection of biological substances, *Biosensors* 5 (2015) 337–363.
- [17] M. Marinescu, *Synthesis and Nonlinear Optical Studies on Organic Compounds in Laser-Deposited Films*, Applied Surface Science, InTech, London, UK, 2018.
- [18] N. Kerru, L. Gummi, S. Maddila, K.K. Gangu, S.B. Jonnalagadda, A review on recent advances in Nitrogen-Containing Molecules and their biological applications, *Molecules* 25 (2020) 1909.
- [19] M. Ordóñez, A. Palillero-Cisneros, V. Labastida-Galván, J.L. Terán-Vázquez, Practical synthesis of 3-(2-arylethylidene)isoindolin-1-ones (analogues of AKS-182) and 3-(2-arylethylidene)isobenzofuran-1(3H)-ones, *Tetrahedron* 76 (2020) 130838.
- [20] A. Palillero-Cisneros, M. Bedolla-Medrano, M. Ordóñez, Efficient PhB(OH)₂-catalyzed one-pot synthesis of 3-substituted isoindolin-1-ones and isobenzofuran-1(3H)-ones under solvent free conditions, *Tetrahedron* 74 (2018) 4174–4181.
- [21] A. Di Mola, L. Palombi, A. Massa, An overview on asymmetric synthesis of 3-substituted isoindolinones, in: *Targets in Heterocyclic Systems*, Vol. 18, 2014. Ed. Chapter 5; Società Chimica Italiana.
- [22] Y. Wang, H. Wang, X. Jiang, Z. Jiang, T. Guo, X. Ji, Y. Li, Y. Li, Z. Li, Synthesis and broad antiviral activity of novel 2-aryl-isoindolin-1-ones towards diverse enterovirus A71 clinical isolates, *Molecules* 24 (2019) 985.
- [23] F. Csende, A. Porkoláb, A review on antibacterial activity of some isoindole derivatives, *Der Pharma Chemica* 10 (2018) 43–50.
- [24] M.H. Norman, D.J. Minick, G.C. Rigdon, Effect of linking bridge modifications on the antipsychotic profile of some phthalimide and isoindolinone derivatives, *J. Med. Chem.* 39 (1996) 149–157.
- [25] I. Sović, S. Jambon, S.K. Pavelić, E. Markova-Car, N. Ilić, S. Depauw, M.-H. David-Cordonnier, G. Karmirski-Zamola, Synthesis, antitumor activity and DNA binding features of benzothiazolyl and benzimidazolyl substituted isoindolines, *Bioorg. Med. Chem.* 26 (2018) 1950–1960.
- [26] L. Mandić, I. Džeba, D. Jadreško, B. Mihaljević, L. Biczókd, N. Basarić, Photophysical properties and electron transfer photochemical reactivity of substituted phthalimides, *New J. Chem.* 44 (2020) 17252–17266.
- [27] J. Trzcionka, A. Noirot, P.-L. Fabre, N. Chouini-Lalanne, Comparative study of the photophysical properties of indoprofen photoproducts in relation with their DNA photosensitizing properties *Photochem. Photobiol. Sci.* 4 (2005) 298–303.
- [28] V. Lhiaubet-Vallet, J. Trzcionka, S. Encinas, M.A. Miranda, N. Chouini-Lalanne, Photochemical and photophysical properties of indoprofen, *Photochem. Photobiol.* 77 (2003) 487–491.
- [29] N. Gao, C. Cheng, C. Yu, E. Hao, S. Wang, J. Wang, Y. Wei, X. Mu, L. Jiao, Facile synthesis of highly fluorescent BF₂ complexes bearing isoindolin-1-one ligand, *Dalton Trans.* 43 (2014) 7121–7127.
- [30] A. Kayet, S. Ajarul, S. Paul, D.K. Maiti, 5-annulation of ketoimines: TFA-Catalyzed construction of Isoindolinone-3-carboxylates and development of photophysical properties, *J. Org. Chem.* 83 (2018) 8401–8409.
- [31] T. Shoji, N. Iida, A. Yamazaki, Y. Ariga, A. Ohta, R. Sekiguchi, T. Nagahata, T. Nagasawa, S. It, Synthesis of phthalimides cross-conjugated with azulene ring,

- and their structural, optical and electrochemical properties, *Org. Biomol. Chem.* 18 (2020) 298–303.
- [32] H. Hwang, H. Ko, S. Park, S.R. Suranagi, D.H. Sin, K. Ch, Fluorine-functionalization of an isoindoline-1,3-dione-based conjugated polymer for organic solar cells, *Org. Electron.* 59 (2018) 247–252.
- [33] Y. Kita, J. Nishida, S. Nishida, Y. Matsui, H. Ikeda, Y. Hirao, T. Kawase, Charge-transfer and arrangement effects on delayed photoluminescence from phthalimide Co-crystals, *Chem. Photo. Chem.* 2 (2018) 42–52.
- [34] A. Gergiev, D. Yordanov, D. Dimov, I. Zhivkov, D. Nazarova, M. Weiter, Azomethine phthalimides fluorescent E-Z photoswitches, *J. Photoch. Photobiol. A* 393 (2020), 112443.
- [35] K.B. Akshaya, A. Varghese, P.L. Lobo, R. Kumari, L. George, Synthesis and photophysical properties of a novel phthalimide derivative using solvatochromic shift method for the estimation of ground and singlet excited state dipole moments, *J. Mol. Liq.* 224 (2016) 247–254.
- [36] S. Kang, S. Lee, W. Yang, J. Seo, M.S. Han, Direct assay of butyrylcholinesterase activity using a fluorescent substrate, *Org. Biomol. Chem.* 14 (2016) 8815–8820.
- [37] M.A. Reyes-González, A. Zamudio-Medina, M. Ordóñez, Practical and high stereoselective synthesis of 3-(arylmethylene)isoindolin-1-ones from 2-formylbenzoic acid, *Tetrahedron Lett.* 53 (2012) 5756–5758.
- [38] M. Ordóñez, G.D. Tibhe, A. Zamudio-Medina, J.L. Viveros-Ceballos, An easy approach for the Synthesis of *N*-Substituted Isoindolin-1-ones, *Synthesis* (2012) 569–574.
- [39] H. Kim, T. Kim, D.G. Lee, S.W. Roh, C. Lee, Nitrogen-centered radical-mediated C-H imidation of arenes and heteroarenes via visible light induced photocatalysis, *Chem. Commun.* 50 (2014) 9273–9276.
- [40] I. Takahashi, T. Kawakami, E. Hirano, M. Kimino, S. Kamimura, T. Miwa, T. Tamura, R. Tazaki, H. Kitajima, M. Hatanaka, K. Isa, S. Hosoi, Application of the mild-condition phthalimidine synthesis with use of 1,2,3-*1H*-benzotriazole and 2-mercaptoethanol as dual synthetic auxiliaries. Effective synthesis of phthalimidines possessing a variety of substituents at 2-position, *Heterocycles* 93 (2016) 557–571.
- [41] H.M. Al-Hazimi, A. El-Faham, M. Ghazzali, K. Al-Farhan, Microwave irradiation: a facile, scalable and convenient method for synthesis of *N*-phthaloylamino acids, *Arabian J. Chem.* 5 (2012) 285–289.
- [42] L. Shi, L. Hu, J. Wang, X. Cao, H. Gu, Highly efficient synthesis of *N*-Substituted isoindolinones and phthalazinones using Pt nanowires as catalysts, *Org. Lett.* 14 (2012) 1876–1879.
- [43] M.J. Frisch, G.W. Trucks, H.B. Schlegel, G.E. Scuseria, M.A. Robb, J.R. Cheeseman, G. Scalmani, V. Barone, G.A. Petersson, H. Nakatsuji, X. Li, M. Caricato, A. Marenich, J. Bloino, B.G. Janesko, R. Gomperts, B. Mennucci, H.P. Hratchian, J. V. Ortiz, A.F. Izmaylov, J.L. Sonnenberg, D. Williams-Young, F. Ding, F. Lipparini, F. Egidi, J. Goings, B. Peng, A. Petrone, T. Henderson, D. Ranasinghe, V. G. Zakrzewski, J. Gao, N. Rega, G. Zheng, W. Liang, M. Hada, M. Ehara, K. Toyota, R. Fukuda, J. Hasegawa, M. Ishida, T. Nakajima, Y. Honda, O. Kitao, H. Nakai, T. Vreven, K. Throssell, J.A. Montgomery, J.E. Peralta, F. Ogliaro, M. Bearpark, J. J. Heyd, E. Brothers, K.N. Kudin, V.N. Staroverov, T. Keith, R. Kobayashi, J. Normand, K. Raghavachari, A. Rendell, J.C. Burant, S.S. Iyengar, J. Tomasi, M. Cossi, J.M. Millam, M. Klene, C. Adamo, R. Cammi, J.W. Ochterski, R.L. Martin, K. Morokuma, O. Farkas, J.B. Foresman, D.J. Fox, Gaussian 09., Revision A.02.02, Gaussian, Inc., Wallingford C.T., 2016.
- [44] A.D. Becke, Density-functional thermochemistry. III. The role of exact exchange, *J. Chem. Phys.* 98 (1993) 5648–5652.
- [45] C. Lee, W. Yang, R.G. Parr, Development of the Colle-Salvetti correlation-energy formula into a functional of the electron density, *Phys. Rev. B* 37 (1988) 785–789.
- [46] E. Cancès, B. Mennucci, J. Tomasi, A new integral equation formalism for the polarizable continuum model: theoretical background and applications to isotropic and anisotropic dielectrics, *J. Chem. Phys.* 107 (1997) 3032–3041.
- [47] B. Mennucci, E. Cancès, J. Tomasi, Evaluation of solvent effects in isotropic and anisotropic dielectrics and in ionic solutions with a unified integral equation method: theoretical bases, computational implementation, and numerical applications, *J. Phys. Chem. B* 101 (1997) 10506–10517.
- [48] J.L. Viveros-Ceballos, C. Cativiela, M. Ordóñez, One-pot three-component highly diastereoselective synthesis of isoindolin-1-one-3-phosphonates under solvent and catalyst free-conditions, *Tetrahedron Asymmetry* 22 (2011) 1479–1484.
- [49] G.D. Tibhe, M. Bedolla-Medrano, C. Cativiela, M. Ordóñez, Phenylboronic acid as efficient and eco-friendly catalyst for the one-pot three-component synthesis of α -Aminophosphonates under solvent free-conditions, *Synlett* 23 (2012) 1931–1936.
- [50] Y. Chen, H. Li, S. Cai, Luminescent *N*-arylphthalimidino derivatives 2- and 4-(1-oxo-1*H*-2,3-dihydroisoindol-2-yl)benzoic acid: examples of a new class of reaction induced crystallization for organic compound, *Chem. Commun.* (2009) 5392–5393.
- [51] I. Azumaya, H. Kagechika, Y. Fujiwara, M. Itoh, K. Yamaguchi, K. Shudo, Twisted intramolecular charge-transfer fluorescence of aromatic amides: conformation of the amide bonds in the excited states, *J. Am. Chem. Soc.* 113 (1991) 2833–2838.
- [52] V. Lhiaubet, F. Gutierrez, F. Penaud-Berruyer, E. Amouyal, J.-P. Deudey, R. Poteau, N. Chouini-Lalanne, N. Paillous, Spectroscopic and theoretical studies of the excited states of fenofibric acid and ketoprofen in relation with their photosensitizing properties, *New J. Chem.* 24 (2000) 403–410.
- [53] W.A. Muriel, R. Morales-Cueto, W. Rodríguez-Córdoba, Unravelling the solvent polarity effect on the excited state intramolecular proton transfer mechanism of the 1- and 2-salicylideneanthyramine. A TD-DFT case study, *Phys. Chem. Chem. Phys.* 21 (2019) 915–928.
- [54] C. Jaramillo-González, R. Morales-Cueto, W. Rodríguez-Córdoba, Absorption and emission spectra of anthracene-9-carboxylic acid in solution within the polarizable continuum model: a long-range corrected time dependent density functional study, in: J.R. Sabin, R. Cabrera-Trujillo (Eds.), *Advances Quantum Chemistry: Concepts of Mathematical Physics in Chemistry: A Tribute to Frank E. Harris-Part B*, 2016, pp. 61–94, 72.
- [55] M.A. Kelterer, A. Mansha, F.J. Iftikhar, Y. Zhang, W. Wang, J.H. Xu, G. Gramp, Computational and experimental studies on the triplet states of various *N*-substituted 4,5,6,7-tetrachlorophthalimides, *J. Mol. Model.* 20 (2014) 2344–2357.
- [56] V. Lhiaubet-Vallet, J. Trzcionka, S. Encinas, M.A. Miranda, N. Chouini-Lalanne, The triplet state of a *N*-Phenylphthalimidine with high intersystem crossing efficiency: characterization by transient absorption spectroscopy and DNA sensitization properties, *J. Phys. Chem. B* 108 (2004) 14148–14153.
- [57] N.J. Turro, V. Ramamurthy, J.C. Scaiano, *Modern Molecular Photochemistry of Organic Compounds*, University Science Books, USA, 2010.
- [58] K.D. Warzecha, H. Gerner, A.G. Griesbeck, Photoinduced decarboxylative benzylation of phthalimide triplets with phenyl acetates: a mechanistic study, *J. Phys. Chem. A* 110 (2006) 3356–3363.
- [59] J.D. Coyle, G.L. Newport, A. Harriman, Nitrogen-substituted phthalimides: fluorescence, phosphorescence, and the mechanism of photocyclization, *J. Chem. Soc. Perkin Trans. I* 2 (1978) 133–137.
- [60] F. Gutierrez, J. Trzcionka, R. Deloncle, R. Poteau, N. Chouini-Lalanne, Absorption and solvatochromic properties of 2-methylisoindolin-1-one and related compounds: interplay between theory and experiments, *New J. Chem.* 29 (2005) 570–578.